Disintegration of Northern Cape iron ores under reducing conditions

W. F. van der Vyver[1], P. C. Pistorius*[2], S. A. Brand[3] and M. Reid[4]

Cracking occurs in the first step of gaseous reduction of hematite iron ore, to magnetite, and can lead to the formation of fine material, with deleterious effects on operation of shaft furnaces. To study this, samples of three ore types from the Northern Cape iron ore field in South Africa, and one blended ore from this region, were studied. The methods were high temperature microscopy (during reduction) and quantification of fines formation following reduction disintegration tests. The ore types do differ significantly with regards to their propensity to form fines. Although disintegration is clearly triggered by reduction, no direct correlation could be established between the degree of reduction and the amount of fines generated. Reduction disintegration increased with higher hydrogen percentages (>5%) in the reduction gas, and at higher temperatures (in the 500–700°C range). Disintegration of the samples decreased at temperatures >750°C. There was no correlation between the presence of gangue minerals and fines formation.

Keywords: Reduction disintegration, Lump ore, Hematite, Gangue

Introduction

Reduction disintegration (low temperature breakdown) in blast furnaces and shaft furnaces occurs during initial reduction of hematite to magnetite. The fundamental cause is the reduction process itself, resulting in a volume expansion and the relieving of stress through the formation of cracks, mainly in the temperature range 500–800°C.[1] The resulting formation of fine material can affect the performance of blast furnaces and shaft furnaces, primarily through diminished gas permeability.

While the molar volume of magnetite is less than that of hematite (Fig. 1),[2,3] expansion is generally observed when hematite is reduced to magnetite. This is associated with specific orientation relationships between the hematite and magnetite,[4] and the formation of porosity within the magnetite reaction product.[5]

Sinter and lump ore both exhibit low temperature breakdown. However, in the case of sinter, specific phases present easier paths for preferential crack propagation, in contrast with lump ore where crack propagation is more random.[6] Nevertheless, the mineralogy of the lump ore does affect breakdown behaviour significantly, with eight mineralogical features (larger grain size, lower porosity, directionality of grain structure and of grain boundaries, poorly contiguous grains, interconnected large pores, layered fine pores and water containing minerals) all contributing to increased reduction disintegration.[1]

The reduction atmosphere significantly affects breakdown, with much less disintegration in atmospheres which contain hydrogen and water vapour, compared with CO/CO_2 atmospheres.[7] This difference was related to the higher nucleation rate of magnetite in the hydrogen containing atmosphere, and 'inward dilation', where the expansion is accommodated by expansion into pre-existing pores.[7]

The specific focus of the present work is on the reduction disintegration of ore from the banded iron formation of the Northern Cape region in South Africa. This ore is a significant export from South Africa (amounting to 27·4 Mt in 2006);[8] it is categorised as a 'Type 2/4' ore in the Goldring[9] scheme (that is, ore hosted in a banded iron formation, with some supergene enrichment).

Northern Cape iron ore generally fares well when tested for reduction disintegration properties. Table 1 lists the reduction disintegration properties of a typical blended Northern Cape iron ore and two (Australian) Brockman iron ores (the latter are also of the Goldring 2/4 type).[9] The results are for the ISO 4696 (Ref. 10) test, which was the basis of the test work in the present work. The much smaller percentage of fines (defined as particles <6·3 mm) which form during reduction illustrates the generally good reduction disintegration properties of the Northern Cape ore. Nevertheless, reduction disintegration remains a concern, notably in the Corex process (at Saldanha Steel in South Africa). For this reason, the work presented here studied whether the subtypes of ore (from different regions

[1]Exxaro Resources, PO box 9229, Pretoria 0001, South Africa. Former graduate student, Dept of Materials Science and Metallurgical Engineering, University of Pretoria
[2]Department of Materials Science and Metallurgical Engineering, University of Pretoria (current address: Department of Materials Science and Engineering, Carnegie Mellon University, Pittsburgh PA 15213, USA)
[3]SGS Advanced Mineralogy Facility (Brisbane), PO Box 1480, Milton, Queensland, 4064, Australia
[4]Faculty of Engineering, University of Wollongong, Wollongong, NSW 2522, Australia

*Corresponding author, email pistorius@cmu.edu

Published by Maney on behalf of the Institute
Received 4 July 2008; accepted 17 October 2008
DOI 10.1179/174328108X393821

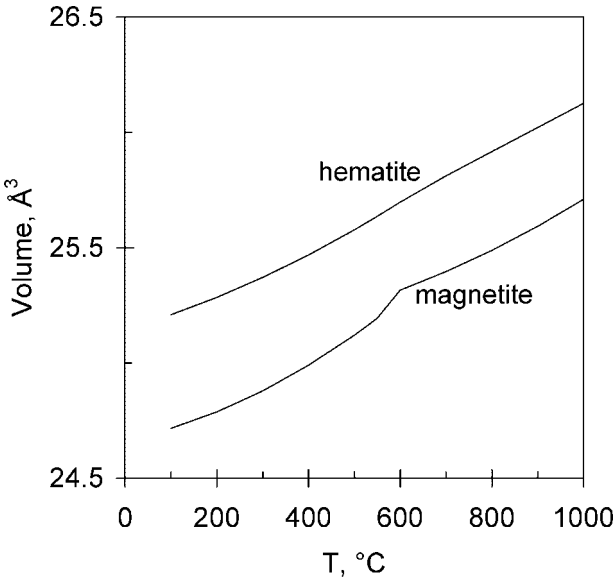

1 Volume, per iron atom, of magnetite and hematite; molar volumes calculated from literature data[2,3] (molar volume of magnetite is smaller than that of hematite, indicating that shrinkage is expected upon reduction of hematite to magnetite, which is opposite of what is practically observed)

within the deposit), and gangue affect reduction disintegration. If these do have a significant effect, lump ore products can be selected to minimise disintegration, for specific applications. In addition, variations on the standard ISO 4696 were considered, with respect to gas composition and temperature. High temperature microscopy was performed, as well as reduction disintegration tests.

Materials and test conditions

Ore types

Four ore types were considered, with chemical compositions (before reduction) as listed in Table 2. The ore type labelled 'Northern Cape STD' is the lump ore as supplied by the mine; it is a mixture of up to seven different ore types to meet the contractually specified chemical analysis and size distribution; the other three types were from specific subareas of the ore deposit. The chemical analyses of the samples before and after testing were used to determine the degree of reduction obtained during testing. Representative micrographs are shown in Fig. 2–5, and the mineralogical properties of the specific ores (that is, excluding the standard mixed type) are summarised below.

Type 2

This contains brecciated, laminated and massive ore particles. Massive particles are laminated on a microscopic scale. In contrast, the laminated particles contain dense, finely crystalline hematite microlaminae alternating with coarser, specularitic mesolaminae. The latter are thicker than 300 μm. The brecciated particles contain dull reddish, porous, earthy laminations, comprising specularitic and earthy hematite. Laminations are wavy and distorted, consistent with soft sediment deformation. The lamellae vary in thickness between 100 and >300 μm. The same textures are observable macroscopically. Ore fragments are commonly cemented by lenticular specularite lathe, silica, phosphates and alumino-silicates. The ore is also relatively porous. Clay minerals are relatively common in the matrix.

Table 1 Comparison of reduction disintegration properties of Northern Cape iron ore and two Brockman ores

Northern Cape	Brockman 1	Brockman 2
11·4	40·0	28·3

Type 4

Brecciated, laminated and massive ore particles are encountered in this ore. All of these particles are characterised by a high concentration of acicular specular hematite.

The massive ore particles consist of both granular and acicular hematite grains and some of the particles exhibit open pore structures up to 300 μm in diameter that are partially filled with slender hematite needles. In laminated particles granular and acicular hematite lamellae alternate, with variations in open porosity as well as higher concentration levels of quartz in the open pores of the hematite matrix. Brecciated ore particles consist of fragments made up of an acicular hematite matrix, cemented together by acicular hematite.

The individual hematite grains range in size from 35 to 50 μm, although longer hematite needles are present in the open pores of the massive ore particle.

Type 5

This is a conglomeratic ore containing angular to subangular ore fragments consisting of specular hematite set in an aluminous matrix. The matrix consists of extremely finely crystalline alumino-silicate groundmass containing euhedral phosphates with lesser quartz and specular hematite. In some instances the matrix phosphates may occur in a cryptocrystalline form, such that they are almost indistinguishable from the enclosing alumino-silicate groundmass.

High temperature microscopy

High temperature microscopy was performed during reduction, to follow crack formation and crack propagation. A high temperature microscope at the University of Wollongong was used. A disc shaped ore sample was heated in the microscope, using an infrared image furnace

Table 2 Chemical analysis of samples before testing (mass percentages)

	Northern Cape STD	Northern Cape 2	Northern Cape 4	Northern Cape 5
Fe (tot)	65·2	67·7	66·9	66·5
Fe_2O_3	92·3	96·7	95·1	94·3
FeO	0·76	0·11	0·47	0·68
Fe°	0·05	0·02	0·06	0·06
CaO	0·055	0·036	0·167	0·028
MgO	0·018	0·022	0·017	0·016
SiO_2	4·06	1·96	1·60	2·86
Al_2O_3	1·20	0·31	1·33	1·01
K_2O	0·149	0·027	0·173	0·018
Na_2O	0·011	0·019	0·020	0·010
TiO_2	0·062	0·021	0·049	0·054
MnO	0·016	0·007	0·013	0·011
P	0·048	0·036	0·068	0·040
S	0·006	0·033	0·007	0·008
C	0·035	0·022	0·036	0·042

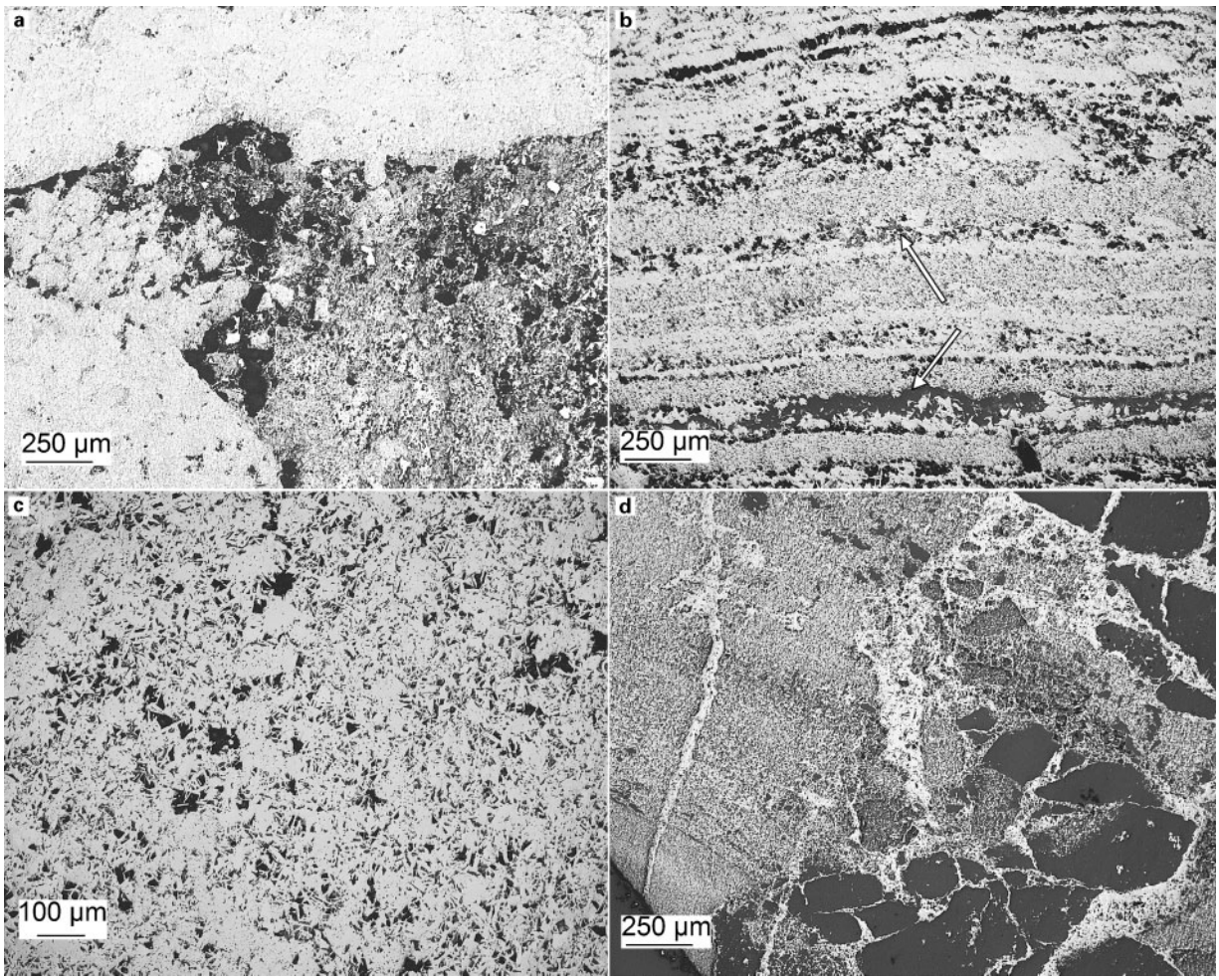

a brecciated earthy hematite ore particle showing alteration to specular hematite (white); *b* typical layered ore particle that exhibits layering due to lamellae of quartz (arrowed), alternating granular hematite (more massive lamellae) and acicular hematite, and open porosity parallel to granular hematite (upper part of micrograph); *c* massive hematite ore particle containing granular and acicular specular hematite, and numerous open pores (black); *d* earthy hematite ore particle showing alteration to specular hematite (white) and containing fragments of quartz (dark areas)

2 Typical backscattered electron images of Northern Cape STD ore blend tested in this work

with an ellipsoid cavity; the microscope has been described in more detail elsewhere.[11] The ore samples were prepared to fit into an alumina crucible, with 10 mm outer diameter, 8 mm inner diameter and 3 mm height. The sample surfaces were polished (with diamond paste) to facilitate imaging. A Lasertec microscope (Model 1LM21) was used, while the video signal was captured using a Snazzi AVIO capture card. Samples were heating under argon (ultra high purity Ar, passed through a Vici He purifier), reaching the test temperature after an hour.

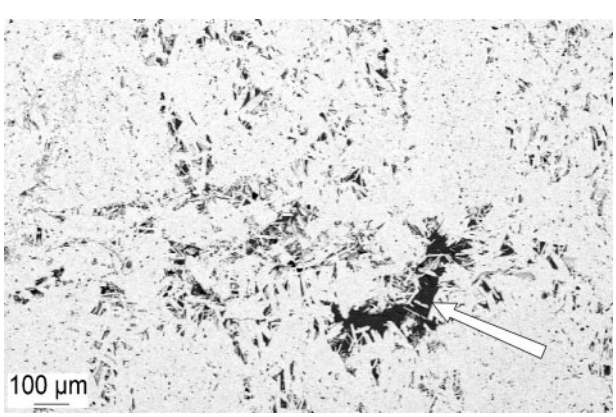

3 Typical backscattered electron images of Northern Cape ore type 2: fracture fillings (arrowed) are chert and alumino-silicates associated with coarse specularite

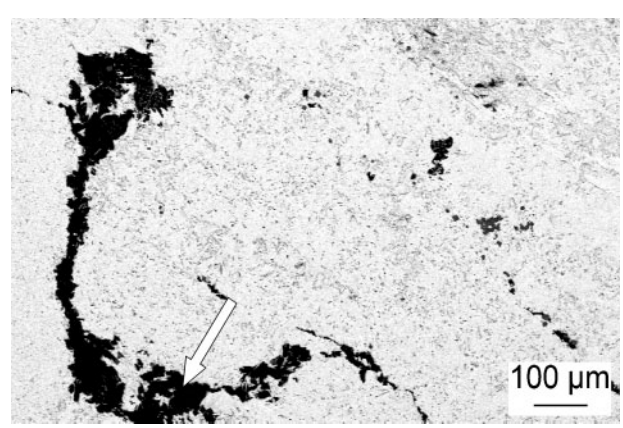

4 Typical backscattered electron images of Northern Cape ore type 5: brecciated ore fragment (variously sized clasts of massive to laminated hematite in matrix of very fine) specular hematite, intergrown with arrowed gangue (chert, alumino-silicates and some phosphate minerals)

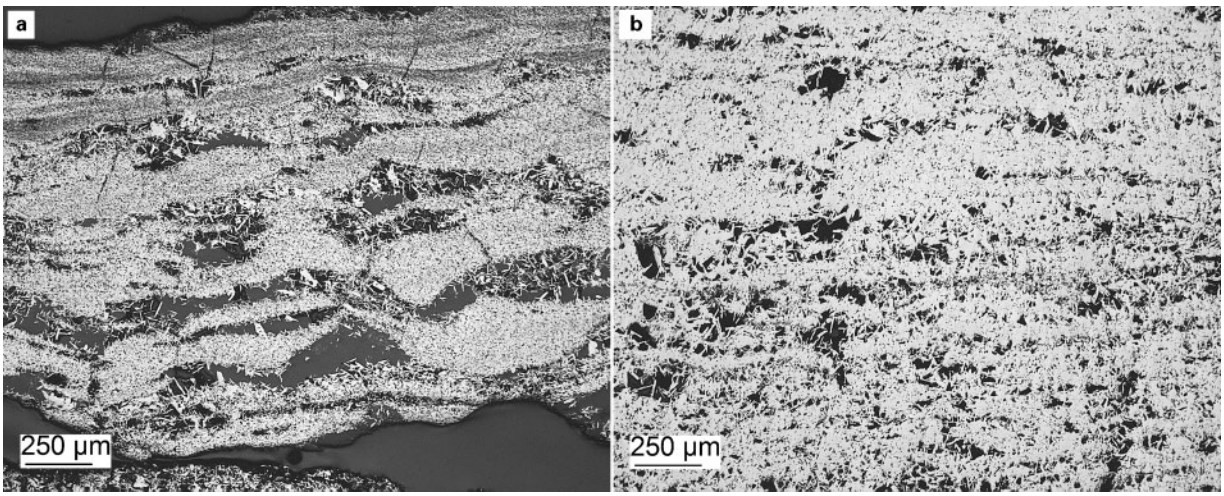

a layered ore particle with irregularly distributed quartz (black) and numerous acicular hematite grains (white) in quartz matrix; *b* laminated ore particle: alternating granular and acicular hematite grains, and open porosity (black)

5 Typical backscattered electron images of Northern Cape ore type 4

Premixed gases (20%CO, 20%CO_2 and 60%N_2; and 5%H_2 in Ar) were the used for reduction. The test conditions are listed in Table 3. The sample was cooled under argon at the end of the reduction period. The gas flowrate was~2 dm^3 min^{-1}.

During the tests, a continuous video recording was made of the entire test. Regions of interest were selected manually, emphasising crack formation and propagation. An objective magnification of 10 times was used. After the tests, the samples were mounted in epoxy resin, polished and coated with gold in a sputter coater, for examination in a JOEL 5800 scanning electron microscope (at the Unit for Microscopy and Micro-Analysis of the University of Pretoria).

Reduction disintegration tests

The reduction disintegration tests were based on ISO 4696,[10] with variations (with regards to gas composition, time and temperature), to test specific effects. In the standard test, a 500 g sample of $-12{\cdot}5+10$ mm material is heated under inert atmosphere (N_2) to 500°C; when the sample reaches 500°C the sample is reduced for one hour in a 20CO–20CO_2–60N_2 mixture, followed by cooling to room temperature under an inert atmosphere. A drum test and sieve analysis is subsequently used to determine the breakdown of the sample.

The full set of test conditions is summarised in Table 4, showing how the reduction conditions were varied relative to the standard, to test specific effects, such as those of temperature, time, and gas composition. Table 4 also lists the amount of fines produced (mass percentage of particles smaller than 6·3 mm), and the degree of reduction for finer and coarser particles. The test numbers which are listed in Table 4 do not form a consecutive series, since the full test programme also included other ore types, and other starting particle size ranges[12] (which are not included here).

Table 3 Test conditions for high temperature microscopy

Sample no.	Ore type	Reduction gas composition (balance Ar), mol.-%	Time at temperature (min); reduction temperature (°C)
1	5	20CO, 20CO_2	60; 500
2	2	20CO, 20CO_2	60; 500
3	4	20CO, 20CO_2	60; 500
6	2	20CO, 20CO_2	60; 500
8	STD	20CO, 20CO_2	60; 500
10	4	20CO, 20CO_2	60; 500
12	2	20CO, 20CO_2	60; 500
13	STD	20CO, 20CO_2	60; 500
14	5	20CO, 20CO_2	60; 500
15	5	20CO, 20CO_2	60; 500
16	STD	20CO, 20CO_2	60; 500
17	4	20CO, 20CO_2	60; 500
18	STD	5H_2	120; 500
19	STD	5H_2	180; 500
20	STD	5H_2	180; 500
21	STD	20CO, 20CO_2	90; 700

Results and discussion

High temperature microscopy

During the high temperature test a video recording was made for the duration of the test. Recordings were evaluated afterwards for crack generation and propagation. Cracks were classified as 'large' (cracks which are likely to lead to failure during tumbling), 'internal' (thin/hairline cracks that would not lead to failure) and 'border' (cracks on the edges of sample that would cause fine particles to spall off the edges of the sample). A summary of the results of the high temperature microscopy is given in Table 5.

During three of the tests the first crack was generated during the heating cycle. In the rest the first crack only appeared 12–30 min after the reduction gas had been introduced. Most of the samples cracked only once. The effect of volume expansion was noticed from crack widening after initial cracking. In an inert atmosphere (argon) no cracking was observed. This confirms that reduction is responsible for cracking.

Propagation of cracks (subsequent to initial crack formation) was only observed in one sample (sample 16) during examination in the high temperature microscope. The reduction time was increased to see whether renewed cracking propagation (due to increased reduction at the crack face) would commence eventually, but this was not found. The influence of reduction gas and temperature on the crack formation and propagation

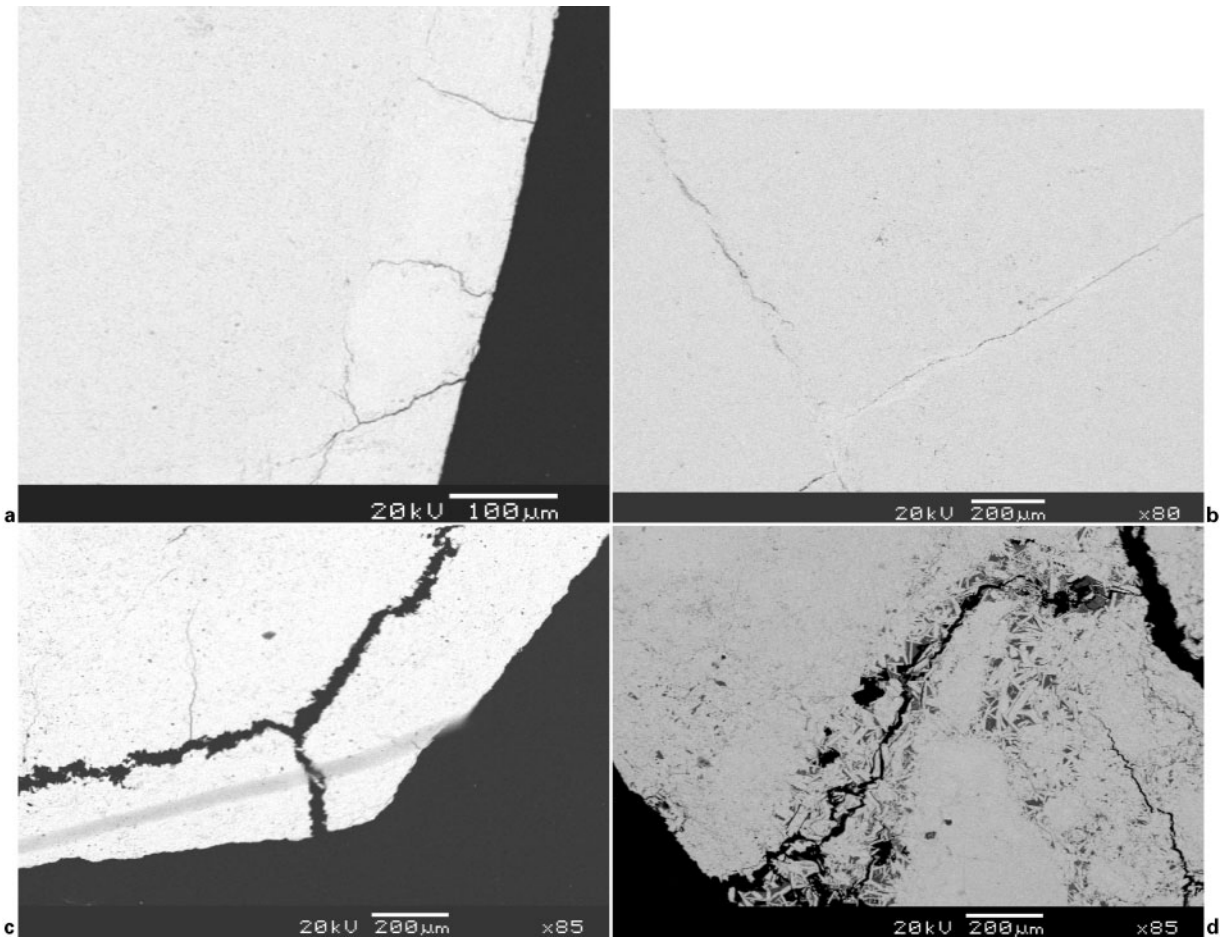

a radial fractures occurring on edges of particles penetrating sample to depth of reduction; *b* internal fractures that occur regularly spaced, at right angles to one another – forming matrix of internal cracks; *c* fractures that occurred perpendicular to edge of sample, where sample has been reduced; *d* fractures associated with gangue minerals or internal structures (internal foliation, open pores, acicular hematite)

6 Typical appearance of cracks after high temperature microscopy (backscattered electron images)

was tested using H_2 as the reduction gas (test 18–20) and increasing the temperature to 700°C (test 21). These did not show any strong effects. It is hence concluded that the reported differences in disintegration behaviour in atmospheres with and without hydrogen[7] and at different temperatures do not involve a fundamental change in mechanism, but rather more subtle changes, possibly including differences in the way in which

Table 4 Reduction disintegration test conditions and results; 'fines amount' is mass percentage of −6·3 mm material after reduction and tumbling

				Reduction per size range, %		
Test no.	Ore type	Changes made from ISO 4696	Fines amount	+6·3 mm	−6·3 mm	Overall
4	STD	No change	9·14	1·73	5·49	2·07
7	2	No change	23·10	0·94	4·11	1·67
9	4	No change	1·08	0·03	12·76	0·17
10	5	No change	10·09	2·37	6·06	2·74
16	STD	t=90 min	16·39	2·27	5·75	2·84
21	STD	t=120 min	17·40	0·78	6·17	1·72
23	STD	T=550°C	13·30	3·05	5·80	3·42
24	STD	T=600°C	12·90	0·82	6·88	1·60
25	STD	T=650°C	12·20	1·63	7·68	2·37
26	STD	T=700°C	12·70	4·60	9·78	5·26
27	STD	5%H_2	9·00	3·41	6·16	3·66
28	STD	10%H_2	12·90	7·42	6·50	7·30
29	STD	T=600°C, t=90 min	13·55	2·12	8·36	2·96
30	STD	T=600°C, t=120 min	23·70	5·12	6·27	5·39
31	STD	T=700°C, t=90 min	11·60	6·25	10·72	6·77
32	STD	T=700°C, t=120 min	19·20	4·25	11·65	5·67
33	STD	T=750°C	8·00	3·19	15·07	4·14
34	STD	T=800°C, t=60 min	5·30	4·63	15·09	5·19

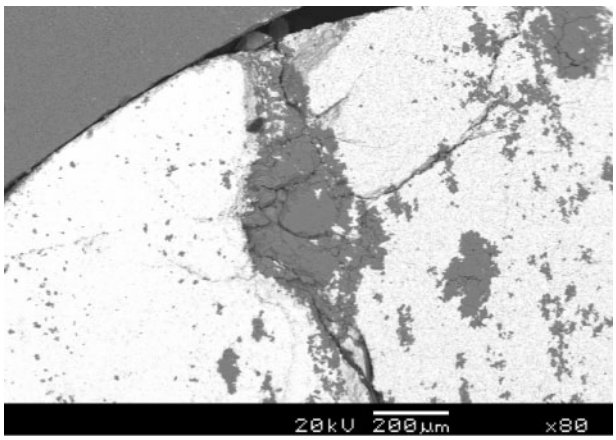

7 Example of crack branching in quartz gangue (darker regions) (backscattered electron image)

porosity develops during reduction.[4] Such subtle effects were not observable in the high temperature microscope as used here.

Table 6 summarises the SEM examination of the samples after reduction in the high temperature microscope. From the SEM investigation the appearance of cracks was classified in four distinct groups, of which examples are shown in Fig. 6.

The results indicate that the presence of gangue minerals alone does not cause fractures to form (this conclusion was also tested with the results of the reduction disintegration tests, as discussed later in this paper). However, the gangue minerals can influence the direction and intensity of fractures. Cracks often branch upon passing through gangue minerals, forming a secondary network of smaller fractures, especially in quartz (*see* Fig. 7 for an example). The secondary fractures do not extend into the surrounding hematite.

Porous samples appear to be less fractured, presumably because the pores are able to accommodate the strain of the volume increase during reduction. This is in line with the classification scheme of Martens *et al.*[1] (regarding susceptibility to reduction disintegration), according to which higher porosity is beneficial for resistance to cracking.

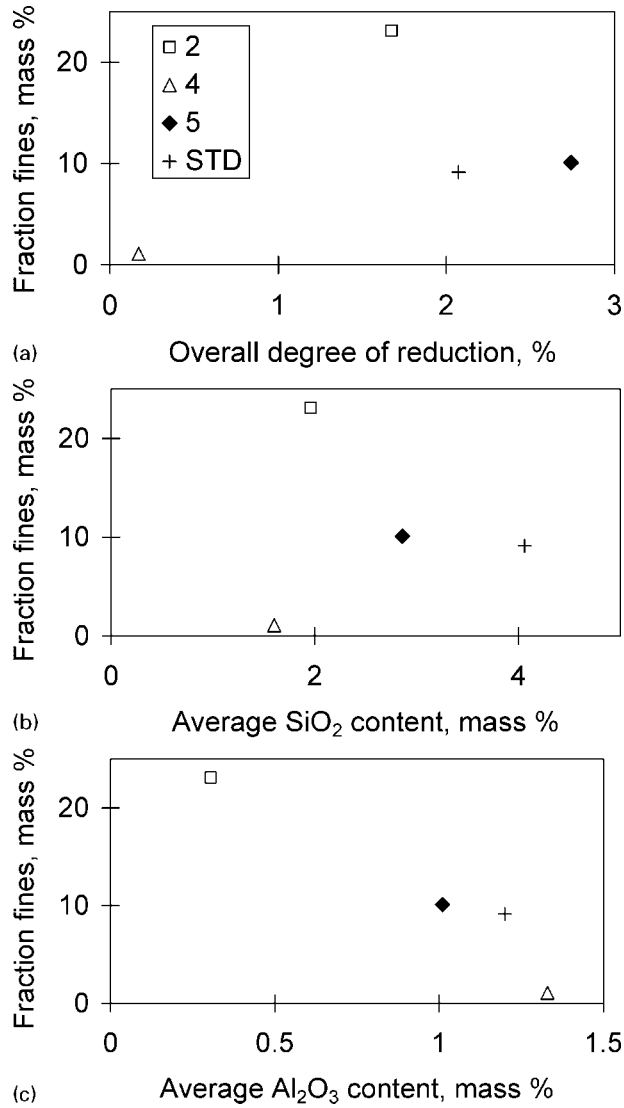

8 For four ore types (indicated by different symbols), there is no obvious correlation of degree of fines formation with *a* degree of reduction, *b* silica content and *c* alumina content (results from standard reduction disintegration test)

Table 5 Summary of cracks observed during and after reduction tests in high temperature microscope

Sample no.	Ore	Time before first crack	No. of large cracks	No. of cracks growing from large cracks	Internal cracks	Border cracks
1	5	17	3	5	6	5
2	2	0	2	3	2	2
3	4	15	0	0	1	3
6	2	0	4	3	2	5
8	STD	26	0	0	3	2
10	4	0	2	0	2	3
12	2	1	1	0	1	1
13	STD	21	1	0	0	4
14	5	16	1	3	1	2
15	5	12	1	2	3	6
16	STD	18	3	5	8	5
17	4	12	2	0	2	3
18	STD	30	3	4	3	5
19	STD	–	0	0	0	0
20	STD	30	3	0	4	2
21	STD	34	0	0	0	2

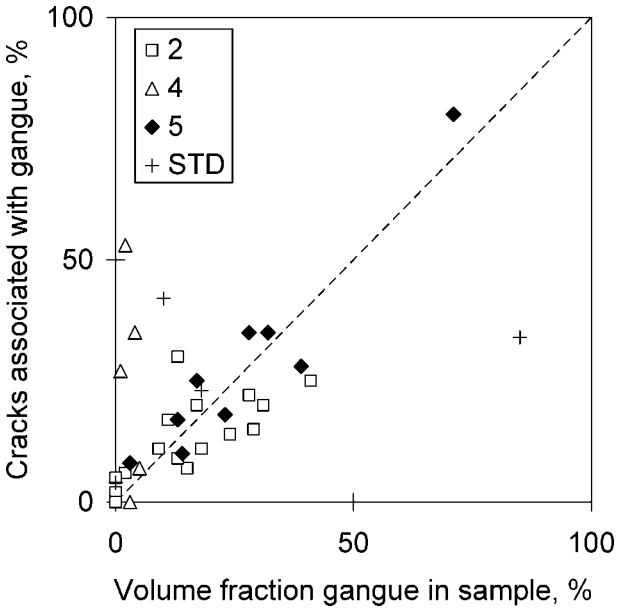

9 **Comparison of degree of association between cracks and gangue, and average volume percentage of gangue, determine by point counting on cross-sections of samples of four ore types after reduction disintegration test (results cluster around broken line, which gives 1 : 1 relationship for random relationship between cracks and gangue)**

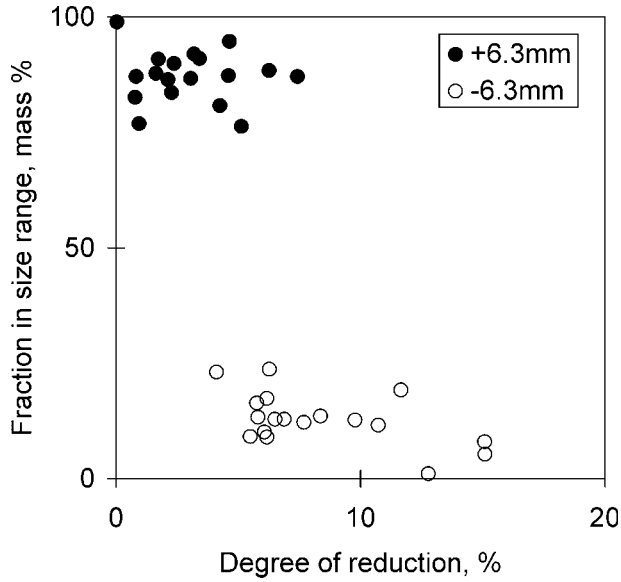

10 **Illustration of lack of clear relationship between degree of reduction and degree of fines formation, for all results given in Table 4**

Reduction disintegration tests

The results from the reduction disintegration tests are summarised in Table 4. Clearly, there are substantial differences between the different ore types. The ores differ regarding their microstructure (as discussed earlier), but also with regards to gangue content and reduction rate. To test whether the latter two factors influence reduction disintegration, plots of the degree of fines formation against ore gangue content and degree of reduction (in the reduction disintegration test) are given in Fig. 8. No relationship is evident from the graphs. High temperature microscopy indicated no strong effect of gangue on cracking; this was also tested with the samples from the reduction disintegration test, by point counting: backscattered electron images were used to quantify the volume fraction of gangue in each field of view, and the fraction of cracks associated with gangue (that is, cracks passing through gangue or along the interface between gangue and iron oxide). The results are shown in Fig. 9, and cluster around the 1 : 1 line; this is the expected behaviour for a random distribution of cracks, with no preference for gangue; this is especially notable in the cases of ore types 2 and 5, which are the ones which showed the greater extent of fines formation. The conclusion is hence that gangue in the ore does not significantly contribute to reduction disintegration. This means that the ore producer cannot influence the reduction disintegration properties of the lump ore product by beneficiating the ore to a product with a different gangue content.

However, the significant difference (in reduction disintegration behaviour) between the ore types from different regions of the mine implies that it would be possible to produce lump ore products with controlled

Table 6 Summary of SEM examination of iron ore samples after reduction under high temperature microscope

Sample no.	Ore	Gangue	Porosity	Fracture type
1	5	Apatite/quartz	Low	Extensive throughout
2	2	–	Variable	Regular network*
3	4	–	Low	Perpendicular to edge
6	2	Quartz	Low	Parallel to foliation
8	STD	–	Low	Perpendicular to edge
10	4	Quartz/muscovite	Low	Parallel to edge
12	2	–	Low	Parallel/perpendicular to edge
13	STD	–	Low	Parallel/perpendicular to edge
14	5	Apatite/quartz	Low	Parallel to edge/regular network
15	5	Al silicates	Low	None observed
16	STD	–	Low	Associated with specularite
17	4	–	Low	Parallel to edge
18	STD	Apatite/quartz	Medium, small pores	Perpendicular/parallel
19	STD	Muscovite/apatite	Low	Parallel
20	STD	Muscovite	Low	Perpendicular
21	STD	Muscovite	Small pores and large infill pores	Perpendicular/parallel

*Regular network – network of fractures that intersect at right angles.

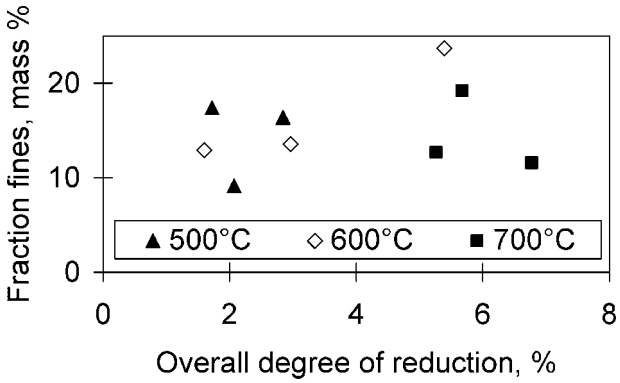

11 Extended reduction at 500, 600 and 700°C (generally giving higher degrees of reduction) does not lead to greater fines formation

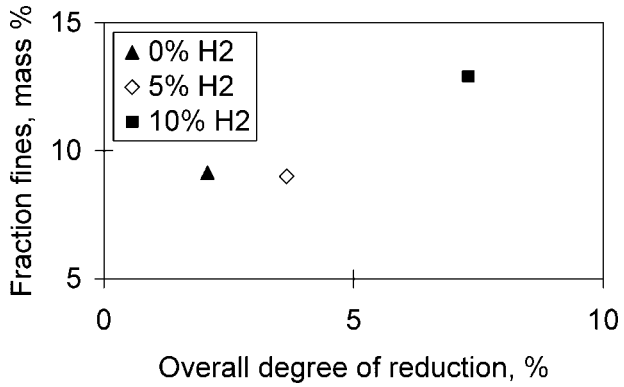

13 Presence of hydrogen in reduction gas gives greater degree of reduction (for tests on STD ore blend), and small increase in fines formation

disintegration properties, by careful selection and blending of material from specific locations in the mine.

While reduction is clearly required for fines formation, there is no simple relationship between the degree of reduction (defined as the fraction of the reducible oxygen which has been removed), and the extent of fines formation. This is demonstrated by Figs. 10–12. Figure 10 plots the mass percentages of the coarse and fine fractions, after all of the tests listed in Table 4, against the degree of reduction of the coarse (+6·3 mm) and fine (−6·3 mm) fractions after each of these tests. The fines are significantly more reduced than the coarse material, as expected from the effect of surface area on reduction rate. What is notable is that there is no strong correlation between the amount of material remaining in the +6·3 mm fraction, and the percentage reduction of this coarse fraction.

Similarly, Fig. 11 shows that, for samples reduced for longer times at temperatures of 500, 600 and 700°C (giving generally greater degrees of reduction), no obvious increase in fines formation is found for higher degrees of reduction. Also, for a wider range of temperatures (Fig. 12), the general increase in the degree of reduction at higher temperatures is not parallelled by an increase in fines formation. The decrease in fines formation >700°C is in line with the suggestion that greater oxide plasticity at these higher temperatures limits fracture.[7]

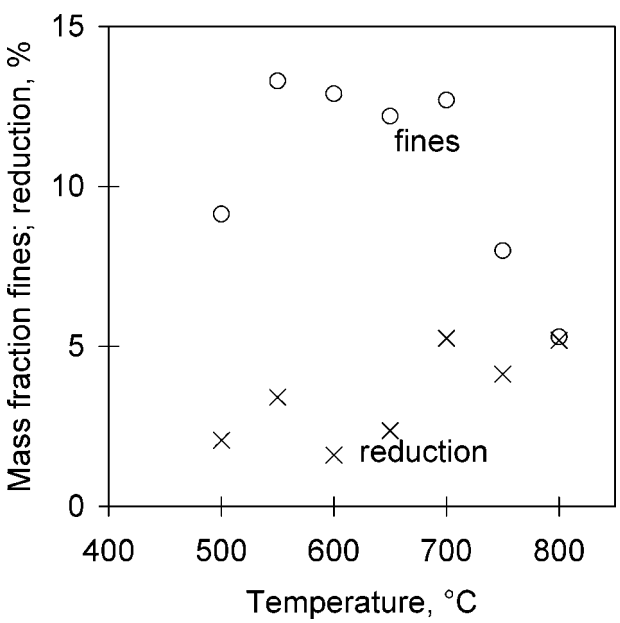

12 Reduction disintegration of STD ore blend decreases above 700°C, even though degree of reduction increases with temperature

Although disintegration is triggered by reduction, no direct correlation could thus be established between the percentage reduction and the percentage fines generated. Clearly other factors in addition to the reduction process influence the degree of reduction disintegration. That is, the differences in disintegration behaviour of different ore types are not just caused by differences in reduction rate. This is in line with the analysis of Martens *et al.*,[1] who noted that several ore properties, including porosity, porosity distribution, and grain structure, influence reduction disintegration behaviour. An implication of this is that more highly reducible ore (which can be a desirable property in some ironmaking applications) need not display greater reduction disintegration.

The results obtained with the H_2 in the reduction gas support this conclusion (*see* Fig. 13). With 5%H_2 in the gas, the degree of reduction is greater, but with no increase in fines formation. With 10%H_2 the degree of reduction doubled, while the fines increased from 9 to 13%.

Conclusions

The content and distribution of gangue has little or no effect on reduction disintegration of Northern Cape iron ore, yet ore types differ considerably with regards to the extent of fines formation, upon reduction of hematite to magnetite.

Reduction conditions (temperature and gas composition) do affect reduction disintegration strongly, but the reduction rate and time for reduction do not have any obvious effects.

These results have practical implications for the way in which ore types are selected or blended for specific ironmaking processes, and the choice of ironmaking process conditions (such as gas composition and temperature profiles).

Acknowledgements

The authors are grateful to Kumba Iron Ore for permission to publish this paper. The authors wish to

acknowledge several persons who contributed to this project: Lourina de Beer, Arno Kleyenstüber, Danie Krige, Mandlakazi Mashao, Stephan Mokwana, Nathan Shago, Leonie Reyneke, Kobus Theron, Christo van Loggerenberg, Gerhard van Niekerk and Kobus Vreugdenburg.

References

1. R. Martens, H. Rausch, H. Serbent and H. Westenberger: *Steel Res.*, 1985, **56**, 147–152.
2. D. Taylor: *Br. Ceram. Soc. Trans. J.*, 1985, **84**, 92–98.
3. D. Taylor: *Br. Ceram. Soc. Trans. J.*, 1985, **84**, 121–127.
4. P. C Hayes and P. Grieveson: *Metall. Trans. B*, 1981, **12B**, 579–587.
5. A. Ünal and A. V. Bradshaw: *Metall. Trans. B*, 1983, **14B**, 743–752.
6. C. E. Loo and N. J. Bristow: *Ironmaking Steelmaking*, 1998, **25**, 287–295.
7. W. M. Husslage, T. Bakker, M. E. Kock and R. H. Heerema: *Miner. Metall. Process.*, 1999, **16**, (3), 23–33.
8. 'Directorate: mineral economics: South Africa's mineral industry 2006/2007', 7; 2007, Pretoria, Department of Minerals and Energy.
9. D. C. Goldring: *Trans. Inst. Min. Metall. B*, 2003, **112B**, B5–B17.
10. 'Iron ores for blast furnace feedstocks – determination of low-temperature reduction-disintegration indices by static method – part 2: reduction with CO and N_2', ISO 4696-2, International Organization for Standardization, 2007.
11. D. Phelan, M. Reid and R. Dippenaar: *Metall. Mater. Trans. A*, 2006, **37A**, 985–994.
12. W. F. van der Vyver: 'Determination of factors influencing the degree of reduction disintegration in Sishen lump ore and the role of gangue minerals in the propagation of cracks', PhD thesis, University of Pretoria, South Africa, 2008.